Angle calculations for the 5-circle surface diffractometer of the Materials Science beamline at the Swiss Light Source

P.R. Willmott[1,*] and C.M. Schlepütz[1]

[1]*Swiss Light Source, Paul Scherrer Institut, CH-5232 Villigen, Switzerland.*

(Dated: June 29, 2007)

Abstract

A step-by-step account is presented describing how to determine the rotational movements of the sample and detector in order to record an (hkl) reflection of a single crystal mounted either in horizontal or vertical geometry on the surface diffractometer of the Materials Science beamline of the Swiss Light Source.

INTRODUCTION

This document explains step-by-step the calculations required to perform reciprocal space movements using the surface diffractometer at the Materials Science beamline of the Swiss Light Source. This is meant as a convenient primer for any interested user, and attempts to bring all the relevant mathematics and physics together in a single document. It draws heavily from the literature, in particular the papers from Busing and Levy [1], Evans-Lutterodt and Tang [2], Vlieg [3, 4], Bunk and Nielsen [5], and Diebel [6].

The diffractometer can be configured in one of two geometries ("vertical" or "horizontal") – which geometry should be used depends on the demands of the experiment.

ROTATION MATRICES

Before we proceed, we briefly summarize active (i.e., rotation of an object, not the coordinate system into the object) right-handed rotations about some angle θ about the x-, y- and z-axes. These are, respectively

$$\mathcal{R}_x^{\theta} = \begin{pmatrix} 1 & 0 & 0 \\ 0 & \cos\theta & -\sin\theta \\ 0 & \sin\theta & \cos\theta \end{pmatrix}; \tag{1}$$

$$\mathcal{R}_y^{\theta} = \begin{pmatrix} \cos\theta & 0 & \sin\theta \\ 0 & 1 & 0 \\ -\sin\theta & 0 & \cos\theta \end{pmatrix}; \tag{2}$$

$$\mathcal{R}_z^{\theta} = \begin{pmatrix} \cos\theta & -\sin\theta & 0 \\ \sin\theta & \cos\theta & 0 \\ 0 & 0 & 1 \end{pmatrix}. \tag{3}$$

The inverse rotations of these $\mathcal{R}^{-1}(\theta)$ are the transposes of the arrays $\mathcal{R}^{T}(\theta)$. Because $\cos\theta = \cos(-\theta)$ and $\sin\theta = -\sin(-\theta)$, these inverse rotations are (obviously) also equal to $\mathcal{R}(-\theta)$.

THE DIFFRACTOMETER

The Newport 5-circle diffractometer is shown in Fig. 1. Of particular note are the three different laboratory coordinate frames. For the calculations described here, the two lower coordinate frames

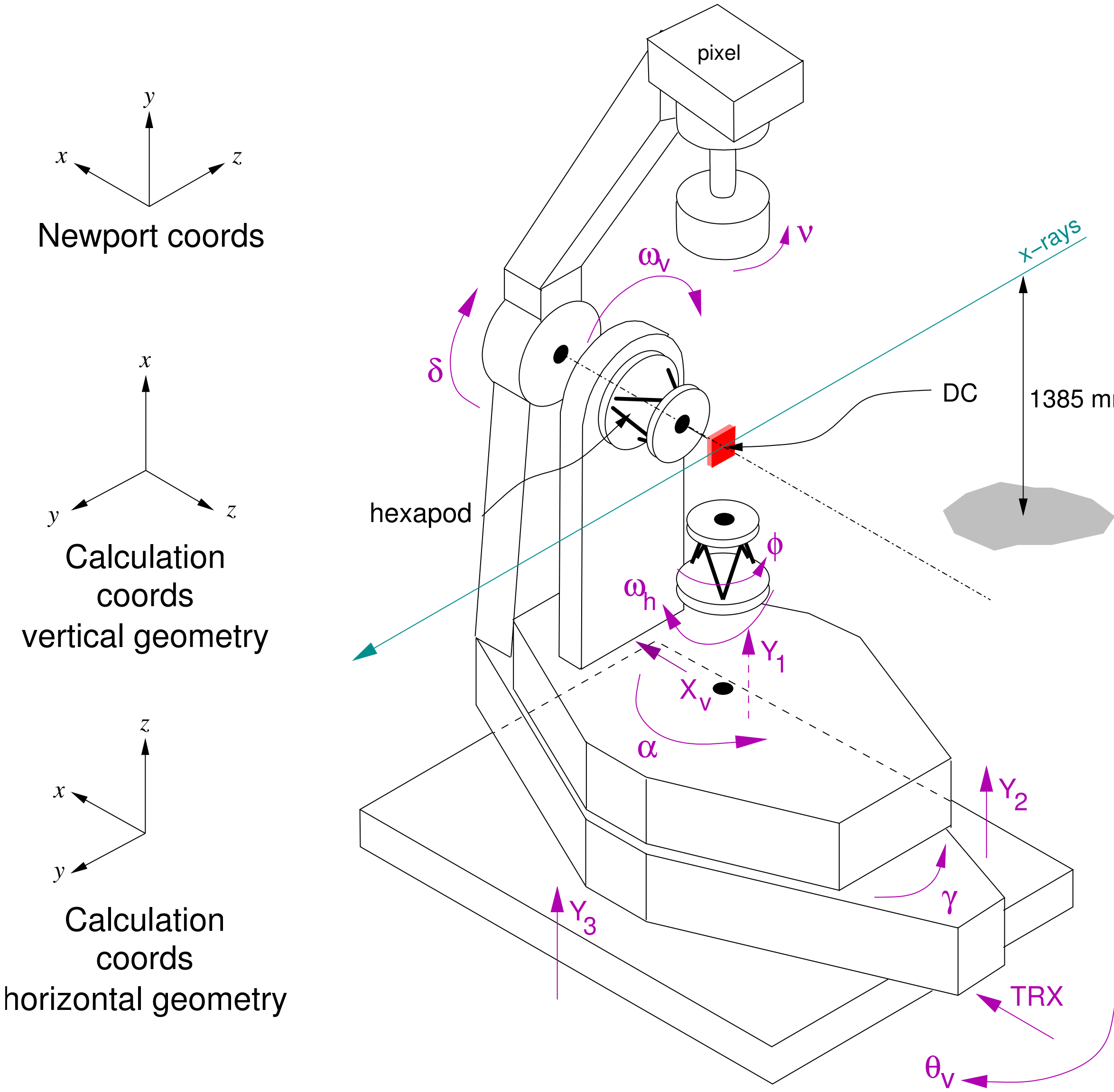

FIG. 1: Schematic figure of the 5-circle (2 sample + 3 detector) Newport diffractometer used at the Surface Diffraction station of the SLS. The sample circles are α and ω_v in the vertical geometry (hexapod axis horizontal) and ω_h and ϕ in the horizontal geometry (hexapod axis vertical), while the detector circles are γ, δ, and ν. All detector and sample motor axes cross at the diffractometer center (DC). Other important motor movements are also shown. Arrow heads point in the positive direction. Three coordinate systems are shown – the Newport Cartesian frame, which tallies with the naming convention of the motors; the calculation frame of reference in the vertical geometry (see also Fig. 2), which is used by both Evans-Lutterodt [2] and Vlieg [3, 4]; and the calculation frame of reference in the horizontal geometry (see also Fig. 7).

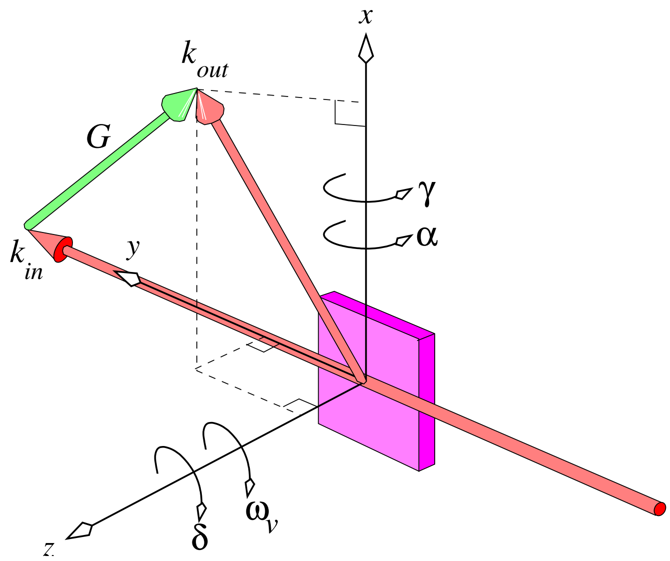

FIG. 2: Schematic figure of the laboratory coordinate system, incoming and outgoing wavevectors $\vec{k}_{in}$ and $\vec{k}_{out}$, the scattering vector $\vec{G}$, and the pertinent motor rotations in the vertical geometry setup of the surface diffractometer.

are relevant – they have both been chosen such that the direct beam points in the positive y-direction and the sample surface normal at 0^o grazing incidence lies along the z-axis. The upper coordinate frame is also shown, as it determines the naming and positive directions of the Newport diffractometer motors (i.e., the direction of the arrows).

In the vertical geometry, motors α, ω_v, γ, δ, and ν are used, while for the horizontal geometry, motors ϕ, ω_h, γ, δ, and ν are used.

VERTICAL GEOMETRY

Geometrical setup

Consider a flat single crystal sample mounted vertically (i.e., with its flat face vertical and its surface normal horizontal), as shown in Fig. 2. Here, the laboratory set of coordinates (x, y, z), are fixed by y being the positive direction of the incident x-ray beam, x being the vertical direction around which both α and γ rotate, z being the horizontal direction around which δ rotates when $\gamma = 0$, and ω_v rotates when $\alpha = 0$. *Note that ω_v and δ are left-handed rotations around the z-axis.*

Using the equations 1 and 3, we therefore obtain for the four circles γ, α, δ, and ω_v, respectively, the rotation matrices Γ, A, Δ, and Ω_v, given by

$$\Gamma = \mathcal{R}_x^{\gamma} = \begin{pmatrix} 1 & 0 & 0 \\ 0 & \cos\gamma & -\sin\gamma \\ 0 & \sin\gamma & \cos\gamma \end{pmatrix}; \tag{4}$$

$$A = \mathcal{R}_x^{\alpha} = \begin{pmatrix} 1 & 0 & 0 \\ 0 & \cos\alpha & -\sin\alpha \\ 0 & \sin\alpha & \cos\alpha \end{pmatrix}; \tag{5}$$

$$\Delta = \mathcal{R}_z^{\delta} = \begin{pmatrix} \cos\delta & \sin\delta & 0 \\ -\sin\delta & \cos\delta & 0 \\ 0 & 0 & 1 \end{pmatrix}; \tag{6}$$

$$\Omega_v = \mathcal{R}_z^{\omega_v} = \begin{pmatrix} \cos\omega_v & \sin\omega_v & 0 \\ -\sin\omega_v & \cos\omega_v & 0 \\ 0 & 0 & 1 \end{pmatrix}, \tag{7}$$

where we note that Δ and Ω_v represent *positive left-handed* rotations.

The relevant rotation matrices for the horizontal geometry are handled in Section , because there a different calculation coordinate orientation is chosen.

Calculating diffractometer angles

The goal of this section is to obtain expressions for the four motor positions (angles) α, ω_v, δ, and γ in terms of the scattering vector in the frame of reference of the crystal surface and the incident and exit angles perpendicular to the crystal surface (referred to as β_{in} and β_{out}, see text below and Fig. 3). We will derive general expressions for these angles, for which specific values will crystallize out, once we define which one of three recording modes we choose to work with, described below.

Our first task is to determine the components X, Y, and Z, of the scattering vector $\vec{G}$ in the laboratory frame of reference. The detector is rotated first by Δ then by Γ (the order of rotation is important, because if the γ-motion is first calculated, this moves the δ-axis out from being coaxial with the z-axis. Therefore, the δ-motion must always be performed first. This also holds for the ω_v (first) and α (second) motions of the sample). The detector is now positined such that it is pointing back along the outgoing, elastically scattered x-ray $\vec{k}_{out}$. We use the fact that, in units of

$2\pi/\lambda$ (for which the magnitude of the incident and scattered wavevectors is then equal to unity), the incoming x-ray beam can be represented by the vector

$$\vec{k}_{in} = \begin{pmatrix} 0 \\ 1 \\ 0 \end{pmatrix} \tag{8}$$

and express the diffraction condition

$$\vec{k}_{out} - \vec{k}_{in} = \vec{G} = \begin{pmatrix} X \\ Y \\ Z \end{pmatrix} \tag{9}$$

by

$$\vec{k}_{out} - \vec{k}_{in} = (\Gamma \cdot \Delta - \mathit{I}) \begin{pmatrix} 0 \\ 1 \\ 0 \end{pmatrix}, \tag{10}$$

where I is the identity matrix. Using our rotation matrices defined above, we therefore obtain

$$\begin{pmatrix} \sin\delta \\ \cos\gamma\cos\delta - 1 \\ \sin\gamma\cos\delta \end{pmatrix} = \begin{pmatrix} X \\ Y \\ Z \end{pmatrix}. \tag{11}$$

We now introduce the vector $\vec{G}_\phi$ given by

$$\vec{G}_\phi = \begin{pmatrix} h_\phi \\ k_\phi \\ l_\phi \end{pmatrix}, \tag{12}$$

which denotes the scattering vector as viewed in the orthonormal Cartesian crystal frame of reference (x_c, y_c, z_c). This frame of reference contains x_c and y_c in the surface of the crystal and therefore z_c is normal to the surface. Note that $\vec{G}_\phi$ does *not* represent the conventional (hkl) Miller indices, because (a) we are using an orthonormal frame of reference (which is not appropriate for hexagonal, triclinic, monoclinic, or rhombohedral crystal systems), and (b) it does not take into account any miscuts of the crystal. This last aspect is dealt with later.

For the angular movements of the sample, α and ω_v, both equal to zero, (x_c, y_c, z_c) and (x, y, z) lie above one another. Let us start in this configuration. In order to satisfy the diffraction condition,

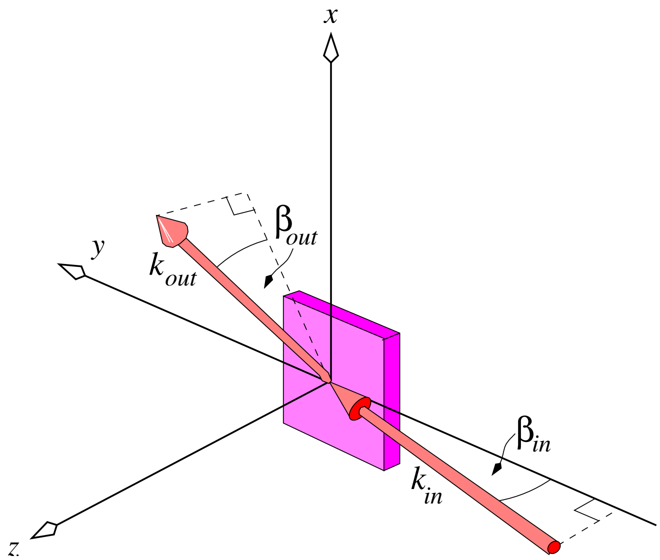

FIG. 3: Schematic of the incident and exit angles β_{in} and β_{out}. In the vertical geometry, β_{in} is equal to α. In the horizontal geometry, β_{in} is equal to ω_h.

we need to first rotate ω_v, then α, which will therefore reposition $\vec{G}_\phi$ into the laboratory-based diffraction condition $\vec{G}$, i.e.,

$$\begin{aligned}\begin{pmatrix} X \\ Y \\ Z \end{pmatrix} &= A \cdot \Omega_v \begin{pmatrix} h_\phi \\ k_\phi \\ l_\phi \end{pmatrix} \\ \Rightarrow \begin{pmatrix} h_\phi \\ k_\phi \\ l_\phi \end{pmatrix} &= \Omega_v^{-1} \cdot A^{-1} \begin{pmatrix} X \\ Y \\ Z \end{pmatrix} \end{aligned} \tag{13}$$

Multiplying out, we obtain

$$\begin{pmatrix} h_\phi \\ k_\phi \\ l_\phi \end{pmatrix} = \Omega_v^{-1} \cdot \begin{pmatrix} X \\ \cos\alpha Y + \sin\alpha Z \\ -\sin\alpha Y + \cos\alpha Z \end{pmatrix} \tag{14}$$

$$= \begin{pmatrix} \cos\omega_v X - \sin\omega_v(\cos\alpha Y + \sin\alpha Z) \\ \sin\omega_v X + \cos\omega_v(\cos\alpha Y + \sin\alpha Z) \\ -\sin\alpha Y + \cos\alpha Z \end{pmatrix}. \tag{15}$$

Consider Fig. 3. In our routines for reciprocal space navigation, three modes are offered, namely a fixed incident x-ray angle ($\beta_{in} = \alpha =$ const.); a fixed exit x-ray angle ($\beta_{out} =$ const.); or

$\beta_{in} = \beta_{out}$.

The momentum transfer perpendicular to the sample surface, l_ϕ, in units of $2\pi/\lambda$, is simply

$$l_\phi = \sin\beta_{in} + \sin\beta_{out}. \tag{16}$$

But from eqns. 11 and 15,

$$\begin{aligned} l_\phi &= -\sin\alpha Y + \cos\alpha Z \\ &= -\sin\alpha(\cos\gamma\cos\delta - 1) + \cos\alpha\cdot\sin\gamma\cdot\cos\delta \\ &= \cos\delta(\sin\gamma\cos\alpha - \cos\gamma\sin\alpha) + \sin\alpha \\ &= \underbrace{\cos\delta\sin(\gamma-\alpha)}_{=\sin\beta_{out}} + \underbrace{\sin\alpha}_{\sin\beta_{in}}. \end{aligned} \tag{17}$$

This is our first condition. We now determine the (squared) magnitude of the in-plane component of $\vec{G}_\phi$. We can predict in advance that this should be independent of ω_v, as this rotation is always normal to the crystal surface. Again, referring back to eqns. 11 and 15, we obtain

$$\begin{aligned} h_\phi^2 + k_\phi^2 &= [\cos\omega_v\cdot X - \sin\omega_v(\cos\alpha\cdot Y + \sin\alpha\cdot Z)]^2 \\ &+ [\sin\omega_v\cdot X + \cos\omega_v(\cos\alpha\cdot Y + \sin\alpha\cdot Z)]^2 \\ &= X^2 + (\cos\alpha\cdot Y + \sin\alpha\cdot Z)^2, \end{aligned} \tag{18}$$

which is indeed independent of ω_v.

The next condition we exploit is the fact that the magnitude of $\vec{G}_\phi$ is equal to that of $\vec{G}$ and that both these must also be independent of ω_v. From eqn. 11, we obtain

$$\begin{aligned} X^2 + Y^2 + Z^2 &= (\sin\delta)^2 + (\cos\gamma\cos\delta - 1)^2 + (\sin\gamma\cos\delta)^2 \\ &= \sin^2\delta + \cos^2\gamma\cos^2\delta - 2\cos\gamma\cos\delta + 1 + \sin^2\gamma\cos^2\delta \\ &= \underbrace{\cos^2\delta\underbrace{(\sin^2\gamma + \cos^2\delta)}_{=1} + \sin^2\delta}_{=1} - 2\cos\gamma\cos\delta + 1 \\ &= 2 - 2\cos\gamma\cos\delta \\ &= -2Y = h_\phi^2 + k_\phi^2 + l_\phi^2. \end{aligned} \tag{19}$$

From eqn. 17, we know that

$$\sin\beta_{out} = \cos\delta\cdot\sin(\gamma - \alpha)$$

$$
\begin{aligned}
&= \cos\delta \cdot (\sin\gamma\cos\alpha - \cos\gamma\sin\alpha) \\
&= \cos\alpha \cdot \sin\gamma\cos\delta - \sin\alpha \cdot \cos\gamma\cos\delta \\
&= \cos\alpha \cdot Z - \sin\alpha \cdot (Y+1). \qquad (20)
\end{aligned}
$$

And by inserting eqn. 19, we obtain

$$\sin\beta_{out} = \cos\alpha \cdot Z - \sin\alpha\left[-\frac{1}{2}(h_\phi^2 + k_\phi^2 + l_\phi^2) + 1\right]. \qquad (21)$$

Remembering that $\sin\alpha = \sin\beta_{in}$, we rearrange eqn. 21 to obtain

$$Z = [\sin\beta_{out} + \sin\beta_{in}(Y+1)] / \cos\alpha. \qquad (22)$$

We now substitute the expressions for Y and Z (eqns. 19 and 22) into eqn. 18:

$$
\begin{aligned}
h_\phi^2 + k_\phi^2 &= X^2 + (\cos\alpha \cdot Y + \sin\alpha \cdot Z)^2 \\
\Rightarrow X &= \pm\left[h_\phi^2 + k_\phi^2 - (\cos\alpha \cdot Y + \sin\alpha \cdot Z)^2\right]^{1/2} \\
&= \pm\left[h_\phi^2 + k_\phi^2 - (\cos\beta_{in} \cdot Y + \sin\beta_{in} \cdot Z)^2\right]^{1/2}. \qquad (23)
\end{aligned}
$$

What have we achieved in deriving eqns. 19 to 23? X, Y, and Z have now been expressed only in terms of h_ϕ, k_ϕ, and l_ϕ (the momentum transfer positions we want to move to in the frame of reference of the crystal surface) and β_{in} and β_{out}, which are still free variables.

We now determine the diffractometer angles α, γ, δ, and ω_v in terms of h_ϕ, k_ϕ, and l_ϕ and X, Y, and Z (which, we have just stated, can themselves be expressed in terms of h_ϕ, k_ϕ, and l_ϕ and β_{in} and β_{out}). From eqn. 11, we directly obtain

$$\sin\delta = X. \qquad (24)$$

We perform a little mathematical jiggerypokery to obtain our expression for γ:

$$
\begin{aligned}
\tan\gamma &= \frac{\sin\gamma}{\cos\gamma} \\
&= \frac{\sin\gamma\cos\delta}{(\cos\gamma\cos\delta - 1) + 1} \\
&= \frac{Z}{Y+1}. \qquad (25)
\end{aligned}
$$

In order to obtain an expression for ω_v, we first define a term

$$K \equiv (\cos\beta_{in} \cdot Y + \sin\beta_{in} \cdot Z), \qquad (26)$$

which we substitute into eqn. 15 to obtain

$$\begin{aligned} h_\phi &= \cos\omega_v \cdot X - \sin\omega_v \cdot K \\ \Rightarrow \cos\omega_v &= \frac{h_\phi + \sin\omega_v \cdot K}{X} \end{aligned}$$

and

$$\begin{aligned} k_\phi &= \sin\omega_v \cdot X + \cos\omega_v \cdot K \\ \Rightarrow \sin\omega_v &= \frac{k_\phi - \cos\omega_v \cdot K}{X}, \end{aligned}$$

and combining these two expressions, we obtain

$$\begin{aligned} \sin\omega_v &= \frac{k_\phi - \frac{h_\phi + \sin\omega_v \cdot K}{X} \cdot K}{X} \\ &= \frac{k_\phi}{X} - \frac{h_\phi \cdot K}{X^2} - \frac{\sin\omega_v \cdot K^2}{X^2} \\ \Rightarrow \sin\omega_v \left(1 + \frac{K^2}{X^2}\right) &= \frac{k_\phi \cdot X}{X^2} - \frac{h_\phi \cdot K}{X^2} \\ \Rightarrow \sin\omega_v &= \frac{k_\phi \cdot X - h_\phi \cdot K}{X^2 + K^2}. \end{aligned} \tag{27}$$

Because ω_v can assume values between $\pm 180^o$, the sine of the desired angle alone does not suffice. So, we now substitute eqn. 27 into eqn. 27, and in a similar manner obtain

$$\cos\omega_v = \frac{h_\phi \cdot X + k_\phi \cdot K}{X^2 + K^2}. \tag{28}$$

From eqns. 27 and 28, we obtain

$$\tan\omega_v = \frac{k_\phi \cdot X - h_\phi \cdot K}{h_\phi \cdot X + k_\phi \cdot K}, \tag{29}$$

which, if we use the `atan2` function, unambiguously determines ω_v.

Finally, of course,

$$\sin\alpha = \sin\beta_{in}. \tag{30}$$

To calculate the diffractometer angles, we need to impose one final constraint on either β_{in} or β_{out}. As we have mentioned already above, there are three available modes one can use to acquire data, namely (a) fixed β_{in}, (b) fixed β_{out}, or (c) $\beta_{in} = \beta_{out}$.

We know from eqn. 16 that

$$l_\phi = \sin\beta_{in} + \sin\beta_{out}. \tag{31}$$

Therefore in case (a), $\beta_{in} = \alpha$ is fixed and hence

$$\begin{aligned} \sin\alpha &= \sin\beta_{in}, \\ \sin\beta_{out} &= l_\phi - \sin\alpha. \end{aligned} \tag{32}$$

For fixed β_{out} [case (b)],

$$\sin\alpha = l_\phi - \sin\beta_{out}, \tag{33}$$

and for $\beta_{in} = \beta_{out}$ [case (c)],

$$\sin\alpha = \frac{l_\phi}{2}. \tag{34}$$

Inserting the appropriate eqn. 32, 33, or 34 into our equations for X, Y, and Z (eqns. 23, 19, and 22, respectively) and then using these in eqns. 24, 25, 27, and 30 we are then able to compute δ, γ, ω_ν, and α, respectively.

Detector rotation, ν

As we can see from Fig. 1, there is a third detector motor movement in addition to δ and γ, namely ν, the rotation of the detector and slits around their symmetry axis. In our setup, we have two active modes of ν-rotation, namely (a) a "static l-projection" (SLP) mode; and (b) a "static footprint projection" (SFP) mode.

SLP mode

The purpose of the ν rotation in the SLP mode is to keep the projection in the planes of the slits and detector of the momentum transfer perpendicular to the crystal surface $\vec{q}_z = \vec{q}_\perp$ parallel to $\vec{\Delta z}$, the opening of the slits in one direction (see Fig. 4). In this manner, the l-direction remains along $\vec{\Delta z}$. This implies that $\vec{\Delta x}$ is always perpendicular to $\vec{q}_\perp$, i.e.,

$$\vec{q}_\perp \cdot \vec{\Delta x} = 0. \tag{35}$$

Let us look at the relevant geometry more closely (Fig. 5). With all motors set to zero, the ν-axis lies along the laboratory y-axis and exhibits a right-handed rotation. The rotation matrix

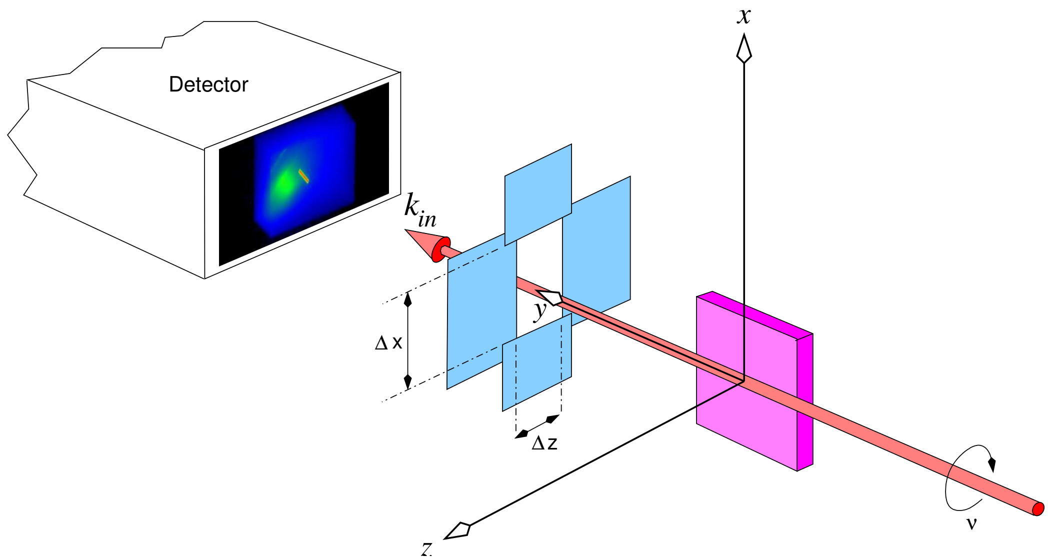

FIG. 4: Schematic figure of the detector and slit system for $\nu = \alpha = \gamma = \delta = 0$. The slit openings are Δx and Δz.

transform for ν, which we call N, is, according to eqn. 2, given by

$$\mathcal{R}_y^{\nu} = \begin{pmatrix} \cos\nu & 0 & \sin\nu \\ 0 & 1 & 0 \\ -\sin\nu & 0 & \cos\nu \end{pmatrix} \equiv N. \tag{36}$$

Also, with all angles set to zero, we can express $\vec{\Delta x}$ and $\vec{q_\perp}$ as

$$\vec{\Delta x} = C_1 \cdot \begin{pmatrix} 1 \\ 0 \\ 0 \end{pmatrix},$$

$$\vec{q}_\perp = C_2 \cdot \begin{pmatrix} 0 \\ 0 \\ 1 \end{pmatrix}.$$

We now move the detector motors to some set of values (ν, δ, γ). It is immediately clear from the schematic shown in Fig. 5 of the scattering vectors as viewed from the perspective of the detector (i.e., along the direction $-\vec{k}_{out}$) that one has to rotate ν in a negative direction to bring $q_\perp$ (the component of $\vec{G}$ perpendicular to the sample surface) parallel to $\vec{\Delta z}$. The three rotations (ν, δ, γ)

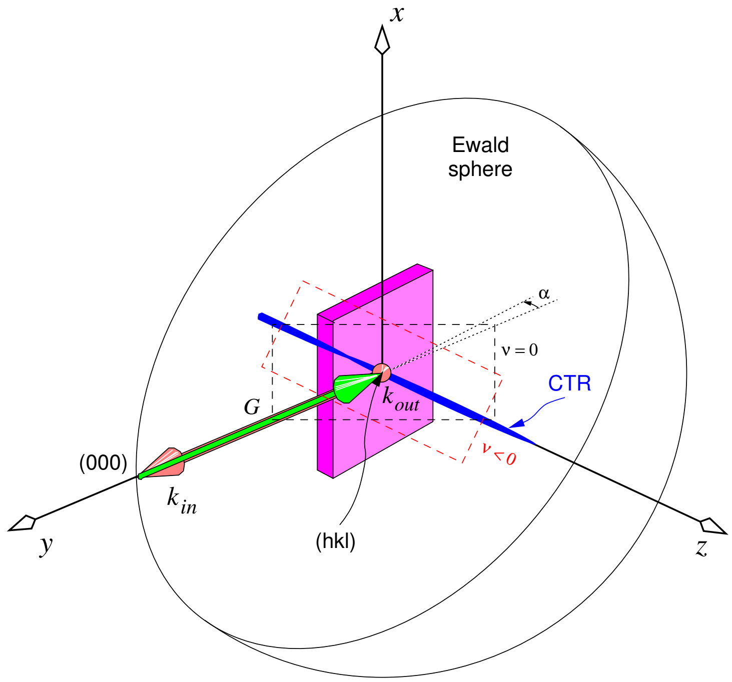

FIG. 5: Schematic figure of the vectors $\vec{k}_{in}$, $\vec{k}_{out}$, and $\vec{G}$, as viewed from the perspective of the detector, which points back along $\vec{k}_{out}$ towards the centre of the diffractometer (hence $\vec{k}_{out}$ is seen here as being "head on"). The vector $\vec{G}$ connects $\vec{k}_{in}$ [at (000)] to $\vec{k}_{out}$ [at (hkl)]. For no rotation of the detector, it is clear that the perpendicular component of $\vec{G}$ is not parallel to the detector frame, which must therefore be rotated in a negative sense to achieve this.

cause $\vec{\Delta x}$ to become

$$\vec{\Delta x} \;=\; \Gamma \Delta N \begin{pmatrix} 1 \\ 0 \\ 0 \end{pmatrix}, \tag{37}$$

where we have dropped the constant C_1 (and will also drop C_2), as the magnitudes of the slit size in the x-direction or the momentum transfer perpendicular to the surface have no bearing on the condition 35.

For non-zero values for α,

$$\vec{q}_{\perp} = A \begin{pmatrix} 0 \\ 0 \\ 1 \end{pmatrix}. \tag{38}$$

Inserting these expressions into eqn. 35, we obtain

$$
\begin{aligned}
A^{-1}\cdot\Gamma\Delta N \begin{pmatrix}1\\0\\0\end{pmatrix} \begin{pmatrix}0\\0\\1\end{pmatrix} &= 0 \\
= A^{-1}\cdot\Gamma\Delta \begin{pmatrix}\cos\nu\\0\\-\sin\nu\end{pmatrix} \begin{pmatrix}0\\0\\1\end{pmatrix} \\
= A^{-1}\cdot\Gamma \begin{pmatrix}\cos\delta\cos\nu\\-\sin\delta\cos\nu\\-\sin\nu\end{pmatrix} \begin{pmatrix}0\\0\\1\end{pmatrix} \\
= A^{-1}\cdot \begin{pmatrix}\cos\delta\cos\nu\\ \cos\gamma(-\sin\delta\cos\nu)+\sin\gamma\sin\nu\\ \sin\gamma(-\sin\delta\cos\nu)-\cos\gamma\sin\nu\end{pmatrix} \begin{pmatrix}0\\0\\1\end{pmatrix} \\
= \begin{pmatrix}\cdots\\ \cdots\\ -\sin\alpha(\cos\gamma(-\sin\delta\cos\nu)+\sin\gamma\sin\nu)+\cos\alpha(\sin\gamma(-\sin\delta\cos\nu)-\cos\gamma\sin\nu)\end{pmatrix} \begin{pmatrix}0\\0\\1\end{pmatrix} \\
\Rightarrow \sin\alpha\cos\gamma\sin\delta\cos\nu - \sin\alpha\sin\gamma\sin\nu - \cos\alpha\sin\gamma\sin\delta\cos\nu - \cos\alpha\cos\gamma\sin\nu \\
= \sin\delta\cos\nu(\sin\alpha\cos\gamma - \cos\alpha\sin\gamma) - \sin\nu(\sin\alpha\sin\gamma + \cos\alpha\cos\gamma) \\
= \sin\delta\cos\nu\sin(\alpha-\gamma) - \sin\nu\cos(\alpha-\gamma) = 0 \\
\Rightarrow -\sin\delta\frac{\sin(\gamma-\alpha)}{\cos(\gamma-\alpha)} = \frac{\sin\nu}{\cos\nu} \\
\Rightarrow \tan\nu = -\tan(\gamma-\alpha)\sin\delta.
\end{aligned} \tag{39}
$$

SFP mode

An incoming x-ray beam incident on a surface at a glancing angle such that it floods the sample will illuminate a stripe across the sample surface. In traditional point-detector scans, a well-defined parallelogram section of this footprint is selected by two sets of slits in the detector arm. When using an area detector, the projection of the footprint is seen as a stripe [see Fig. 6(a)]. The orientation of this stripe on the pixel image depends on the angle of the footprint on the sample, as viewed from the perspective of the detector. Hence, in Fig. 6(b), the angle of the detector in the

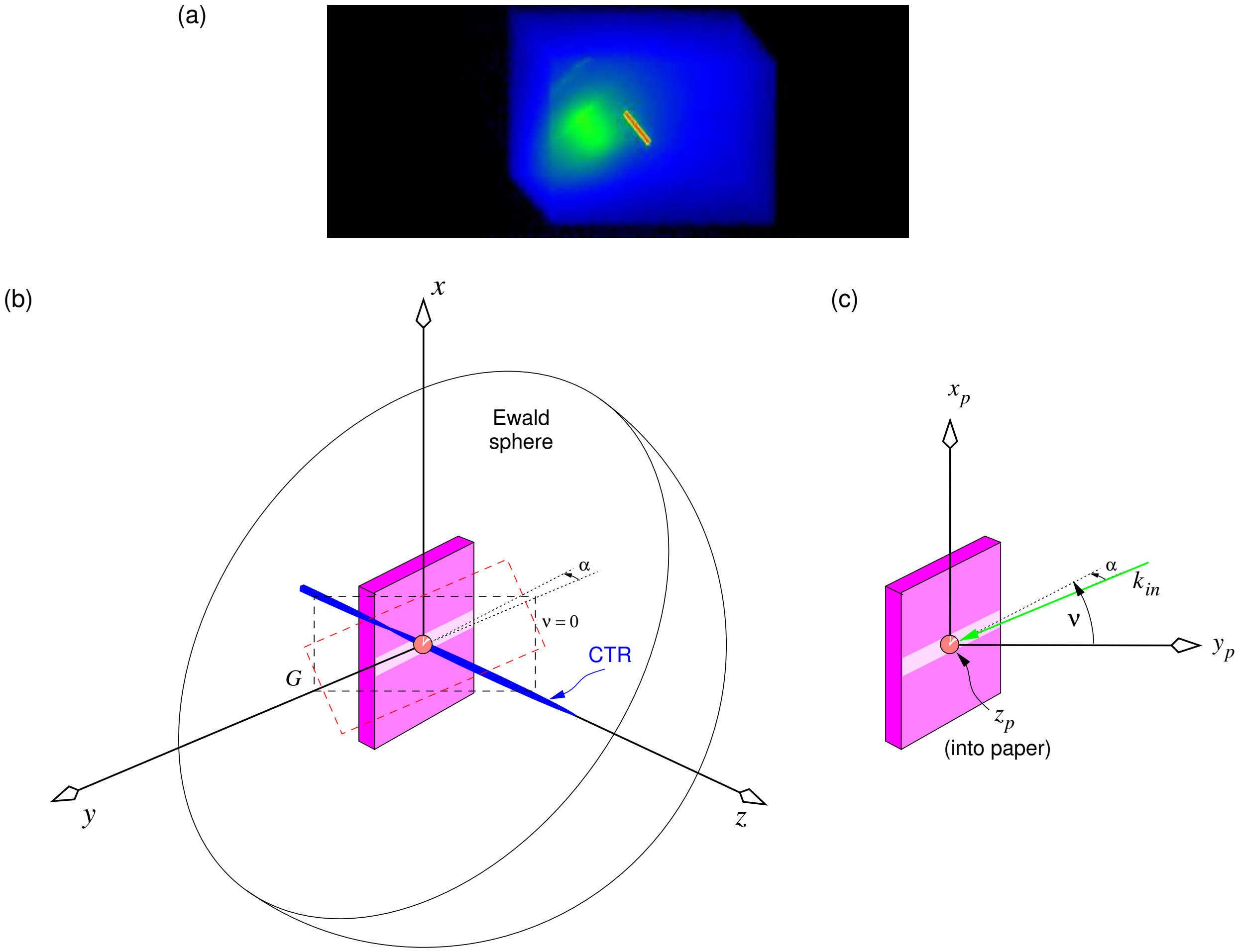

FIG. 6: (a) The footprint of the grazing-incidence beam on the sample is seen as a stripe on the area pixel detector. (b) The unrotated detector [black dashed box] sees this footprint at an angle which depends on the position of the detector and the tilt if the sample to the direct beam [i.e., the δ, γ and α angles]. The footprint can be made to be parallel to the long edge of the area detector by rotating it around ν [red dashed box]. (c) The coordinate system (x_p, y_p, z_p) used to calculate the ν-rotation for the SFP mode is defined by, and stationary with respect to, the detector.

$\nu = 0$ position (dashed black box) is not parallel to the footprint (light purple stripe).

Hence, if either no ν-rotation or the SLP mode is chosen, the projection of the footprint is seen to rotate within the pixel frame as one moves up a CTR. For example, if there is no detector-axis rotation, the footprint stripe is seen to be parallel to the short sides of the detector frame close to the base of the CTR (low γ values), while at the maximum accessible l, for which $\delta = 0$, the footprint stripe is parallel to the long sides of the detector frame. Under such conditions, therefore, the detector slits must either be kept open at least to a square with edges equal in size to the sample footprint stripe, or else must be constantly varied from l-position to l-position in order to accommodate the apparent footprint rotation from the perspective of the detector, which is a complicated and normally impractical solution.

In the SFP mode, this problem is circumvented by rotating the ν-axis such that the long sides of the detector frame remain parallel to the footprint [the red dashed box in Fig. 6(b)]. This therefore allows the user to close down the vertical slits (i.e., those with their edges parallel to the long sides of the detector frame) to values only marginally larger than the width of the footprint, which means stray background signal (such as that produced by the incoming beam passing through a beryllium dome) can be kept to a minimum.

We now derive the expression for the ν-rotation for any given α, δ, and γ values. We begin by assuming that $\alpha = 0$, and define a Cartesian coordinates system (x_p, y_p, z_p) that is fixed in the detector frame of reference [see Fig. 6(c)]. In this frame of reference, it should be clear that ν is equal to the inverse tangent of the component of $-k_{in}$ in the x_p-direction divided by that in the y_p-direction, i.e.,

$$\nu \;=\; \tan^{-1}\left(\frac{k_{in}^{x_p}}{k_{in}^{y_p}}\right). \tag{40}$$

To move $-k_{in}$ into the frame of reference of the pixel detector, we imagine that we begin with the detector looking directly down the incoming beam (z_p colinear with $-k_{in}$). We now rotate γ in a negative sense around x_p, and then δ in a positive sense around y_p. This is exactly the opposite order of rotation compared to that described before in our angle calculations. This is because we are now rotating the whole diffractometer and incoming x-ray beam in the frame of reference of the detector, and *not* rotating the detector in the frame of reference of the diffractometer.

Referring back to our general expressions for rotation matrices (eqns. 1 to 3), the relevant rotation matrices are therefore

$$\Gamma_p = \mathcal{R}_{x_p}^{-\gamma} \;=\; \begin{pmatrix} 1 & 0 & 0 \\ 0 & \cos\gamma & \sin\gamma \\ 0 & -\sin\gamma & \cos\gamma \end{pmatrix}; \tag{41}$$

$$\Delta_p = \mathcal{R}_{y_p}^{\delta} \;=\; \begin{pmatrix} \cos\delta & 0 & \sin\delta \\ 0 & 1 & 0 \\ -\sin\delta & 0 & \cos\delta \end{pmatrix}. \tag{42}$$

The incident beam in the detector frame of reference k'_{in} is therefore

$$\begin{aligned}
k'_{in} &= \Delta_p \Gamma_p k_{in} \\
&= \Delta_p \begin{pmatrix} 1 & 0 & 0 \\ 0 & \cos\gamma & \sin\gamma \\ 0 & -\sin\gamma & \cos\gamma \end{pmatrix} \begin{pmatrix} 0 \\ 0 \\ 1 \end{pmatrix} |k| \\
&= \Delta_p \begin{pmatrix} 0 \\ \sin\gamma \\ \cos\gamma \end{pmatrix} |k| \\
&= \begin{pmatrix} \cos\delta & 0 & \sin\delta \\ 0 & 1 & 0 \\ -\sin\delta & 0 & \cos\delta \end{pmatrix} \begin{pmatrix} 0 \\ \sin\gamma \\ \cos\gamma \end{pmatrix} |k| \\
&= \begin{pmatrix} \sin\delta\cos\gamma \\ \sin\gamma \\ \cos\delta\cos\gamma \end{pmatrix} |k|.
\end{aligned} \tag{43}$$

Using the x_p- and y_p-components of k'_{in} in eqn. 40, we obtain

$$\nu = \tan^{-1}\left(\frac{\sin\delta\cos\gamma}{\sin\gamma}\right).$$

Until now, we have assumed that $\alpha = 0$. For nonzero α, we merely need to rotate by $\gamma - \alpha$ instead of γ, and our equation becomes

$$\nu = \tan^{-1}\left(\frac{\sin\delta\cos(\gamma-\alpha)}{\sin(\gamma-\alpha)}\right). \tag{44}$$

HORIZONTAL GEOMETRY

Geometrical setup

Consider a flat single crystal sample mounted horizontally (i.e., with its flat face horizontal and its surface normal vertical), as shown in Fig. 7. Here, the laboratory set of coordinates (x,y,z), are fixed by y being the positive direction of the incident x-ray beam, z being the vertical direction around which γ rotates and ϕ also rotates, as long as ω_h (which determines the angle of incidence of the incoming beam) is set to zero. x is the horizontal direction around which ω_h rotates and

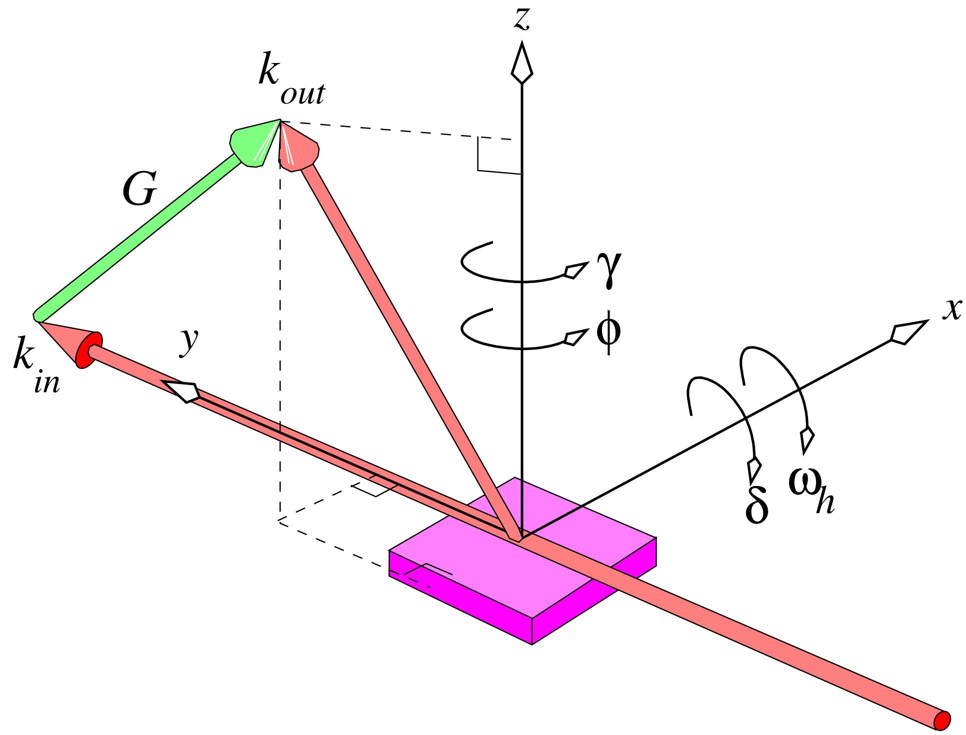

FIG. 7: Schematic figure of the laboratory coordinate system, incoming and outgoing wavevectors $\vec{k}_{in}$ and $\vec{k}_{out}$, the scattering vector $\vec{G}$, and the pertinent motor rotations in the horizontal geometry setup of the surface diffractometer.

also δ rotates when $\gamma = 0$. *Note that in this geometry, all motor rotations exhibit positive right-handedness*.

Using the equations 2 and 3, we therefore obtain for the four circles γ, ϕ, δ, and ω_h, respectively, the rotation matrices Γ, Φ, Δ, and Ω_h, given by

$$\Gamma = \mathcal{R}_z^{\gamma} = \begin{pmatrix} \cos\gamma & -\sin\gamma & 0 \\ \sin\gamma & \cos\gamma & 0 \\ 0 & 0 & 1 \end{pmatrix}; \tag{45}$$

$$\Phi = \mathcal{R}_z^{\phi} = \begin{pmatrix} \cos\phi & -\sin\phi & 0 \\ \sin\phi & \cos\phi & 0 \\ 0 & 0 & 1 \end{pmatrix}; \tag{46}$$

$$\Delta = \mathcal{R}_x^{\delta} = \begin{pmatrix} 1 & 0 & 0 \\ 0 & \cos\delta & -\sin\delta \\ 0 & \sin\delta & \cos\delta \end{pmatrix}; \tag{47}$$

$$\Omega_h = \mathcal{R}_x^{\omega_h} \; = \; \begin{pmatrix} 1 & 0 & 0 \\ 0 & \cos\omega_h & -\sin\omega_h \\ 0 & \sin\omega_h & \cos\omega_h \end{pmatrix}. \tag{48}$$

Calculating diffractometer angles

The incoming x-ray beam (in units of $2\pi/\lambda$) is now represented by the vector

$$\vec{k}_{in} = \begin{pmatrix} 0 \\ 1 \\ 0 \end{pmatrix}. \tag{49}$$

We now essentially go through the same procedure as described above for the vertical geometry. We begin with the diffraction condition, eqn. 9

$$\vec{k}_{out} - \vec{k}_{in} \; = \; \vec{G} = \begin{pmatrix} X \\ Y \\ Z \end{pmatrix}$$

and move the detector to the required position for capturing the diffracted beam:

$$\begin{aligned} \Rightarrow \vec{k}_{out} - \vec{k}_{in} \; &= \; (\Gamma \cdot \Delta - I) \begin{pmatrix} 0 \\ 1 \\ 0 \end{pmatrix} \\ &= \; \Gamma \begin{pmatrix} 0 \\ \cos\delta \\ \sin\delta \end{pmatrix} - \begin{pmatrix} 0 \\ 1 \\ 0 \end{pmatrix} \\ &= \; \begin{pmatrix} -\cos\delta \sin\gamma \\ \cos\delta \cos\gamma - 1 \\ \sin\delta \end{pmatrix} = \begin{pmatrix} X \\ Y \\ Z \end{pmatrix}. \end{aligned} \tag{50}$$

Again, we now rotate the crystal into the diffraction condition, i.e.,

$$\begin{pmatrix} X \\ Y \\ Z \end{pmatrix} \; = \; \Omega_h \cdot \Phi \begin{pmatrix} h_\phi \\ k_\phi \\ l_\phi \end{pmatrix}$$

$$\Rightarrow \begin{pmatrix} h_\phi \\ k_\phi \\ l_\phi \end{pmatrix} = \Phi^{-1} \cdot \Omega_h^{-1} \begin{pmatrix} X \\ Y \\ Z \end{pmatrix}. \tag{51}$$

Multiplying out, we obtain

$$\begin{aligned} \begin{pmatrix} h_\phi \\ k_\phi \\ l_\phi \end{pmatrix} &= \Phi^{-1} \cdot \begin{pmatrix} X \\ \cos\omega_h Y + \sin\omega_h Z \\ -\sin\omega_h Y + \cos\omega_h Z \end{pmatrix} \\ &= \begin{pmatrix} \sin\phi(\cos\omega_h Y + \sin\omega_h Z) + \cos\phi X \\ \cos\phi(\cos\omega_h Y + \sin\omega_h Z) - \sin\phi X \\ \cos\omega_h Z - \sin\omega_h Y \end{pmatrix}. \end{aligned} \tag{52}$$

Referring back to Fig. 3 for the vertical geometry and remembering that the incident angle $\beta_{in} = \omega_h$, we again obtain eqn. 16

$$l_\phi = \sin\beta_{in} + \sin\beta_{out} \tag{53}$$

for the momentum transfer perpendicular to the substrate surface. But from eqns. 50 and 52, we know that

$$\begin{aligned} l_\phi &= -\sin\omega_h Y + \cos\omega_h Z \\ &= -\sin\omega_h(\cos\delta\cos\gamma - 1) + \cos\omega_h \sin\delta \\ &= \underbrace{\sin\omega_h}_{\sin\beta_{in}} + \underbrace{\sin\delta\cos\omega_h - \cos\delta\sin\omega_h\cos\gamma}_{\sin\beta_{out}}. \end{aligned} \tag{54}$$

We again determine the squared magnitude of the in-plane component of $\vec{G}_\phi$, which we have argued is independent of ϕ, as this rotation is always normal to the crystal surface. Referring once more back to eqns. 50 and 52, we obtain

$$\begin{aligned} h_\phi^2 + k_\phi^2 &= [\sin\phi(\cos\omega_h Y + \sin\omega_h Z) + \cos\phi X]^2 \\ &+ [\cos\phi(\cos\omega_h Y + \sin\omega_h Z) - \sin\phi X]^2 \\ &= X^2\cos^2\phi + \sin^2\phi(\cos\omega_h Y + \sin\omega_h Z)^2 + 2X\cos\phi\sin\phi(\cos\omega_h Y + \sin\omega_h Z) \\ &+ X^2\sin^2\phi + \cos^2\phi(\cos\omega_h Y + \sin\omega_h Z)^2 - 2X\cos\phi\sin\phi(\cos\omega_h Y + \sin\omega_h Z) \\ &= X^2 + (\cos\omega_h Y + \sin\omega_h Z)^2, \end{aligned} \tag{55}$$

which, as predicted, is independent of ω_h. Remembering that $\omega_h = \beta_{in}$, we rearrange eqn. 55 to obtain

$$X = \pm\left[h_\phi^2 + k_\phi^2 - (\cos\beta_{in}\cdot Y + \sin\beta_{in}\cdot Z)^2\right]^{1/2}. \tag{56}$$

We use the negative solution, as we will see later in eqn. 60 that this is needed in order to make the δ- and γ–circles move in a positive direction.

The next condition we exploit is the fact that the magnitude of $\vec{G}_\phi$ is equal to that of $\vec{G}$ and that both these must also be independent of ω_h. From eqn. 50, we obtain

$$\begin{aligned} X^2+Y^2+Z^2 &= \cos^2\delta\sin^2\gamma + \cos^2\delta\cos^2\gamma + 1 - 2\cos\delta\cos\gamma + \sin^2\delta \\ &= \cos^2\delta + 1 - 2\cos\delta\cos\gamma + \sin^2\delta \\ &= 2 - 2\cos\gamma\cos\delta \\ &= -2Y = h_\phi^2 + k_\phi^2 + l_\phi^2 \\ \Rightarrow Y &= -(h_\phi^2 + k_\phi^2 + l_\phi^2)/2. \end{aligned} \tag{57}$$

From eqn. 50 and the far right-hand term of eqn. 54, we obtain

$$\begin{aligned} \sin\beta_{out} &= \cos\omega_h\cdot\sin\delta - \sin\omega_h\cdot\cos\delta\cdot\cos\gamma \\ &= \cos\omega_h\cdot Z - \sin\omega_h(Y+1) \\ &= \cos\omega_h\cdot Z - \sin\beta_{in}(Y+1) \\ \Rightarrow Z &= [\sin\beta_{out} + \sin\beta_{in}(Y+1)]/\cos\omega_h. \end{aligned} \tag{58}$$

So, with equations 56, 57, and 58, we have been able to express the three orthogonal components of the scattering vector in the laboratory frame (X, Y, and Z) in terms of the components of the same scattering vector in the crystal frame (h_ϕ, k_ϕ, and l_ϕ) and the angles β_{in} and β_{out}.

Our next step is to solve for the diffractometer angles γ, δ, φ, and ω_h. From eqn. 50,

$$\begin{aligned} \tan\gamma &= \frac{\sin\gamma}{\cos\gamma} \\ &= \frac{\sin\gamma\cos\delta}{\cos\gamma\cos\delta - 1 + 1} \\ &= \frac{-X}{Y+1}. \end{aligned} \tag{59}$$

Note that $\tan\gamma$ depends on the individual signs of X and $Y+1$, hence we use the quadrant-specific `atan2` function in ANSI C.

Again using eqn. 50, we immediately obtain

$$\begin{aligned}\sin\delta &= Z;\\ \cos\delta &= \frac{-X}{\sin\gamma}\end{aligned}$$

and hence

$$\tan\delta = \frac{Z\cdot\sin\gamma}{-X}. \tag{60}$$

For determining ϕ, we define

$$K = \cos\beta_{in}\cdot Y + \sin\beta_{in}\cdot Z. \tag{61}$$

Using this definition, we obtain from eqn. 52

$$\begin{aligned}h_\phi &= \sin\phi\cdot K + \cos\phi\cdot X\\ \Rightarrow \cos\phi &= \frac{h_\phi - \sin\phi\cdot K}{X}\\ k_\phi &= \cos\phi\cdot K - \sin\phi\cdot X\\ \Rightarrow \sin\phi &= \frac{-k_\phi + \cos\phi\cdot K}{X}.\end{aligned}$$

By following the same procedure as we have already detailed for the equivalent case in the vertical geometry, we obtain by inserting these two expressions into one another

$$\tan\phi = \frac{h_\phi\cdot K - k_\phi\cdot X}{h_\phi\cdot X + k_\phi\cdot K}. \tag{62}$$

Again, we need one additional constraint in order to solve for the four physical angles γ, δ, ω_h and ϕ, which, as before for the vertical geometry, we obtain by defining three possible recording modes, i.e., β_{in} fixed; β_{out} fixed; or $\beta_n = \beta_{out}$.

For β_{in} fixed, this implies that $\omega_h \equiv \beta_{in}$ is fixed. Therefore

$$\sin\beta_{out} = l_\phi - \sin\omega_h. \tag{63}$$

Similarly, for β_{out} fixed,

$$\sin\omega_h = \sin\beta_{in} = l_\phi - \sin\beta_{out}. \tag{64}$$

And finally for $\beta_n = \beta_{out}$,

$$\sin\beta_{in} = \sin\beta_{out} = l_\phi/2. \tag{65}$$

We are now able to uniquely calculate all angles by inserting eqns. 63, 64 and 65 into our expressions for X, Y, and Z.

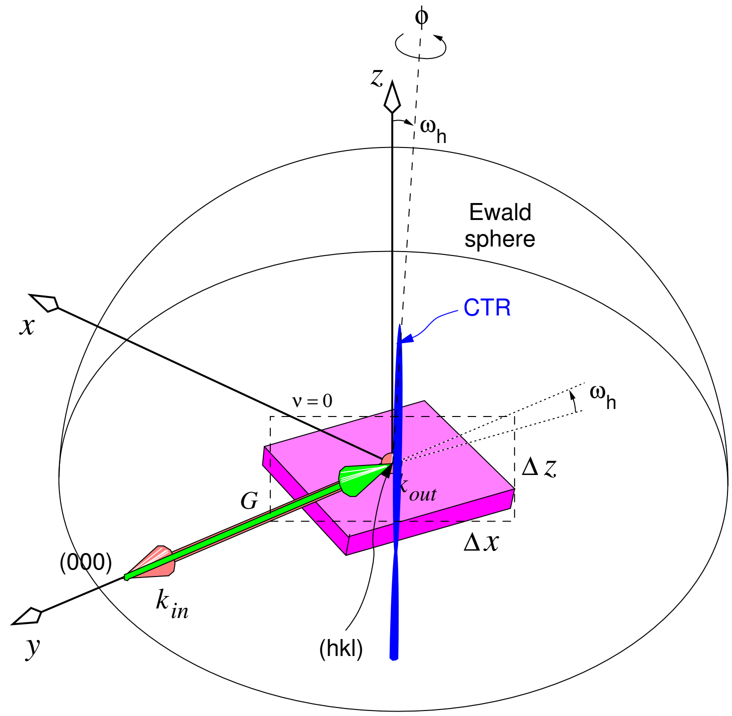

FIG. 8: Schematic figure of the vectors $\vec{k}_{in}$, $\vec{k}_{out}$, and $\vec{G}$, as viewed from the perspective of the detector, which points back along $\vec{k}_{out}$ towards the centre of the diffractometer (hence $\vec{k}_{out}$ is seen here as being "head on"). The vector $\vec{G}$ connects $\vec{k}_{in}$ [at (000)] to $\vec{k}_{out}$ [at (hkl)].

Detector rotation, ν

There are also the same two active detector rotation modes available for the horizontal geometry. The first mode, i.e., the static l-projection (SLP) mode, produces only small adjustments of ν for modest incident angles ω_h. The second (SFP) mode invokes ν-rotations which are essentially identical to those for the same mode in the vertical geometry. Both modes are now detailed.

SLP mode

If we consider Fig. 8, it should be clear that the detector "sees" CTRs that are almost vertical, i.e., parallel to the short edge of the detector frame, independent of the angles δ and γ. This is only approximately true, and rotation of ν is necessary for non-zero incident angles ω_h.

Using the same arguments as those for the SLP mode in the vertical geometry, we require that

$$\vec{q}_{\perp} \cdot \vec{\Delta x} = 0, \tag{66}$$

in other words, the CTR and the long edge of the detector are perpendicular to one another. As in the vertical geometry (eqn. 36), with all the motors set to zero, the ν-axis lies along the laboratory y-axis and exhibits a right-handed rotation, i.e.,

$$\mathcal{R}_y^{\nu} = \begin{pmatrix} \cos\nu & 0 & \sin\nu \\ 0 & 1 & 0 \\ -\sin\nu & 0 & \cos\nu \end{pmatrix} \equiv N.$$

Also, with all angles set to zero, we can express $\vec{\Delta x}$ and $\vec{q}_{\perp}$ as

$$\begin{aligned} \vec{\Delta x} &= C_1 \cdot \begin{pmatrix} 1 \\ 0 \\ 0 \end{pmatrix}, \\ \vec{q}_{\perp} &= C_2 \cdot \begin{pmatrix} 0 \\ 0 \\ 1 \end{pmatrix}. \end{aligned}$$

The three detector rotations (ν, δ, γ) cause $\vec{\Delta x}$ to become

$$\vec{\Delta x} = \Gamma \Delta N \begin{pmatrix} 1 \\ 0 \\ 0 \end{pmatrix}, \tag{67}$$

where we will again drop the constant C_1 and C_2.

For non-zero values for ω_h,

$$\vec{q}_{\perp} = \Omega_h \begin{pmatrix} 0 \\ 0 \\ 1 \end{pmatrix}. \tag{68}$$

Inserting these expressions into eqn. 66, we obtain

$$\Omega_h^{-1} \cdot \Gamma \Delta N \begin{pmatrix} 1 \\ 0 \\ 0 \end{pmatrix} \begin{pmatrix} 0 \\ 0 \\ 1 \end{pmatrix} = 0$$

$$= \Omega_h^{-1} \cdot \Gamma\Delta \begin{pmatrix} \cos\nu \\ 0 \\ -\sin\nu \end{pmatrix} \begin{pmatrix} 0 \\ 0 \\ 1 \end{pmatrix}$$

$$= \Omega_h^{-1} \cdot \Gamma \begin{pmatrix} \cos\nu \\ \sin\delta\sin\nu \\ -\cos\delta\sin\nu \end{pmatrix} \begin{pmatrix} 0 \\ 0 \\ 1 \end{pmatrix}$$

$$= \Omega_h^{-1} \cdot \begin{pmatrix} \cos\gamma\cos\nu - \sin\gamma\sin\delta\sin\nu \\ \sin\gamma\cos\nu + \cos\gamma\sin\delta\sin\nu \\ -\cos\delta\sin\nu \end{pmatrix} \begin{pmatrix} 0 \\ 0 \\ 1 \end{pmatrix}$$

$$= \begin{pmatrix} \cdots \\ \cdots \\ -\sin\omega_h \sin\gamma\cos\nu - \sin\omega_h \cos\gamma\sin\delta\sin\nu - \cos\omega_h \cos\delta\sin\nu \end{pmatrix} \begin{pmatrix} 0 \\ 0 \\ 1 \end{pmatrix} = 0$$

$$\Rightarrow \sin\nu(\sin\omega_h \cos\gamma\sin\delta) = -\sin\gamma\sin\omega_h \cos\nu$$

$$\Rightarrow \tan\nu = \frac{-\sin\gamma\sin\omega_h}{\sin\omega_h \cos\gamma\sin\delta + \cos\omega_h \cos\delta} \tag{69}$$

SFP mode

The expression for the SFP mode is identical to that given by eqn. 44, except that now the correction for the incident angle to the surface is not a subtraction of α from γ, but a subtraction of ω_h from δ, i.e.,

$$\nu \;=\; \tan^{-1}\left(\frac{\sin(\delta-\omega_h)\,\cos\gamma}{\sin\gamma}\right). \tag{70}$$

* philip.willmott@psi.ch

[1] W. R. Busing and H. A. Levy, Acta Crystal. **22**, 457 (1967).

[2] K. W. Evans-Lutterodt and M.-T. Tang, J. Appl. Crystallogr. **28**, 318 (1995).

[3] E. Vlieg, J. Appl. Crystallogr. **30**, 532 (1997).

[4] E. Vlieg, J. Appl. Crystallogr. **31**, 198 (1998).

[5] O. Bunk and M. M. Nielsen, J. Appl. Crystallogr. **37**, 216 (2004).

[6] J. Diebel, *Representing attitude: Euler angles, unit quaternions, and rotation vectors* (2006), http://ai.stanford.edu/ diebel/attitude/attitude.pdf.